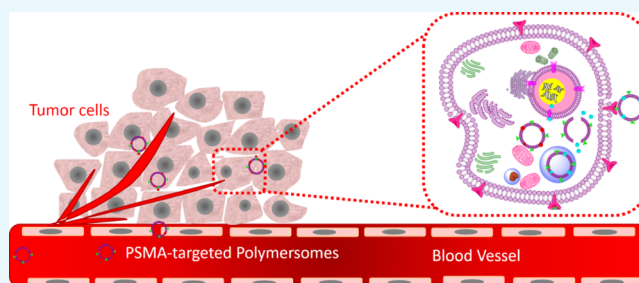


Prostate-Specific Membrane Antigen Targeted Polymersomes for Delivering Mocetinostat and Docetaxel to Prostate Cancer Cell Spheroids

Fataneh Karandish,[†] Manas K. Haldar,^{†,§} Seungyong You,[‡] Amanda E. Brooks,[†] Benjamin D. Brooks,[†] Bin Guo,^{†,||} Yongki Choi,[‡] and Sanku Mallik^{*,†}

[†]Department of Pharmaceutical Sciences and [‡]Department of Physics, North Dakota State University, 1401 Albrecht Blvd., Fargo, North Dakota 58102, United States

ABSTRACT: Prostate cancer cells overexpress the prostate-specific membrane antigen (PSMA) receptors on the surface. Targeting the PSMA receptor creates a unique opportunity for drug delivery. Docetaxel is a Food and Drug Administration-approved drug for treating metastatic and androgen-independent prostate cancer, and mocetinostat is a potent inhibitor of class I histone deacetylases. In this study, we prepared reduction-sensitive polymersomes presenting folic acid on the surface and encapsulating either docetaxel or mocetinostat. The presence of folic acid allowed efficient targeting of the PSMA receptor and subsequent internalization of the polymeric vesicles in cultured LNCaP prostate cancer cell spheroids. The intracellular reducing agents efficiently released docetaxel and mocetinostat from the polymersomes. The combination of the two drug-encapsulated polymersome formulations significantly ($p < 0.05$) decreased the viability of the LNCaP cells (compared to free drugs or control) in three-dimensional spheroid cultures. The calculated combination index value indicated a synergistic effect for the combination of mocetinostat and docetaxel. Thus, our PSMA-targeted drug-encapsulated polymersomes has the potential to lead to a new direction in prostate cancer therapy that decreases the toxicity and increases the efficacy of the drug delivery systems.



1. INTRODUCTION

In the United States, prostate cancer is the most common carcinoma in men after skin malignancy.¹ Approximately one in seven men will be diagnosed with prostate cancer during their lifetime.² Surgery, radiation, and conventional chemotherapy are the common treatment options. However, in conventional chemotherapy, the anticancer drugs distribute throughout the body and destroy the normal cells as well as cancer cells, causing cytotoxicity and side effects.^{3,4} To increase the efficacy, a long-circulating drug delivery vehicle that recognizes the cancer cells and releases the contents in the cytosol is required. Various nanocarriers (e.g., polymeric micelles, liposomes, nanoparticle-aptamer, polymersomes, and nanoparticle delivering miRNA, siRNA, and cell-penetrating peptide) have been developed for cancer treatment with varying degrees of success.^{5–12} Polymersomes are robust bilayer vesicles prepared from synthetic, amphiphilic block copolymers. The incorporation of polyethylene glycol (PEG) as the hydrophilic block renders the vesicles long circulating.¹³ The bilayer of the polymersomes encapsulates hydrophobic drugs, and the aqueous core incorporates the hydrophilic drugs.¹³ The nanocarriers usually escape through the leaky vasculature and accumulate in the tumor due to the poor lymphatic drainage (termed as the enhanced permeation and retention (EPR) effect).¹⁴ After passive targeting by the EPR effect, interactions with a specific

receptor on the cell surface enable cellular internalization of the nanocarriers via endocytosis.⁴

Prostate-specific membrane antigen (PSMA) is an extracellular transmembrane glycoprotein overexpressed in the malignant prostate tissue¹⁵ and is responsible for the uptake of folic acid.¹⁶ The androgen-dependent LNCaP prostate cancer cell line expresses the PSMA receptor. However, the PC3 cells lose the expression of PSMA as the cancer progresses from the androgen-dependent to the androgen-independent stage.^{17,18} Capromab pendetide (PSMA antibody) is the only prostate cancer imaging agent approved by the US Food and Drug Administration (FDA).¹⁹ Mocetinostat (MGCD0103) is an aminophenyl benzamide histone deacetylase (class I enzymes) inhibitor. Mocetinostat induces hyperacetylation of histones and leads to apoptosis and cell cycle arrest in cancer cell lines and the human tumor xenograft mouse model.²⁰ Currently, mocetinostat is used in the clinical trials as a monotherapy or as an adjuvant in many malignancies, although the mechanism is poorly understood.²¹ Docetaxel belongs to the taxoid family and is extracted from the European yew tree.²² It inhibits microtubule depolymerization, causes mitotic spindle poisoning, and blocks mitoses.²³ The US FDA approved docetaxel in 2004 for the

Received: July 15, 2016

Accepted: October 25, 2016

Published: November 16, 2016

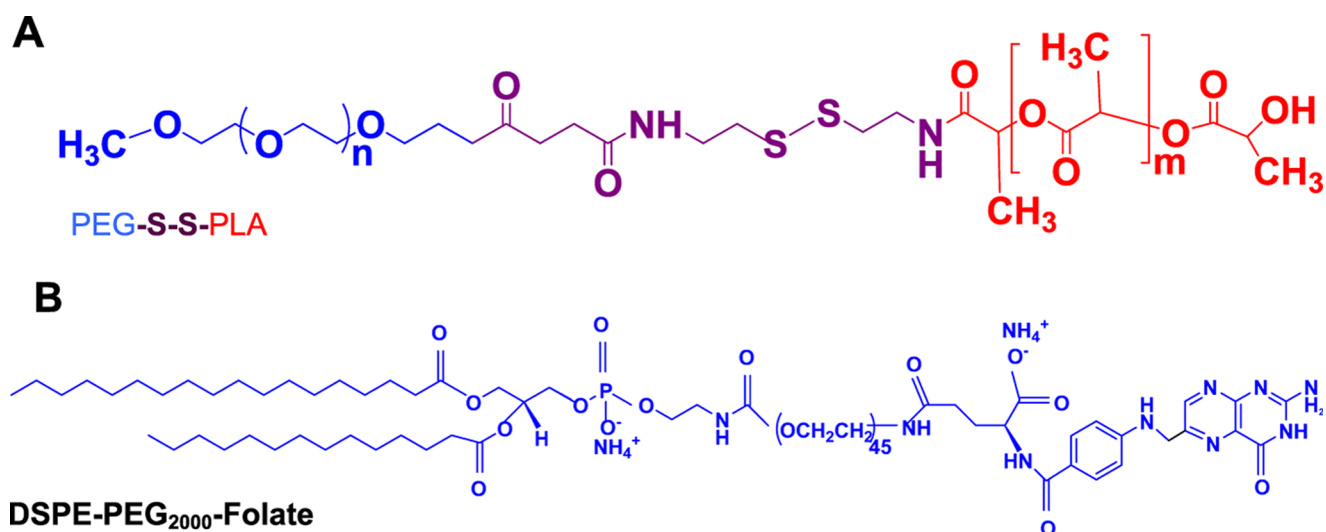


Figure 1. Structures of the synthesized amphiphilic polymer (A) and the commercially available distearoylphosphatidylethanolamine (DSPE)–PEG–folate lipid (B).

Table 1. Size and Polydispersity Index (PDI) of the Polymersomes

formulations	particle size Z-average (nm)	zeta potential (mV)	PDI
polymeromes	216 ± 4	−5.92 ± 0.52	0.1 ± 0.03
PSMA-targeted polymersomes	238 ± 2	−4.87 ± 0.36	0.16 ± 0.02
polymeromes encapsulating mocetinostat	220 ± 3	−5.02 ± 0.42	0.22 ± 0.02
PSMA-targeted polymersomes encapsulating mocetinostat	271 ± 3	−8.06 ± 1.89	0.2 ± 0.01
polymeromes encapsulating carboxyfluorescein	226 ± 7	−12.88 ± 2.4	0.3 ± 0.05
polymeromes encapsulating docetaxel	218 ± 2	−5.36 ± 0.22	0.28 ± 0.01
PSMA-targeted polymersomes encapsulating carboxyfluorescein	220 ± 4	−6.77 ± 1.89	0.3 ± 0.03
PSMA-targeted polymersomes encapsulating docetaxel and carboxyfluorescein	251 ± 4	−4.75 ± 1.02	0.24 ± 0.03

treatment of metastatic, androgen-independent prostate cancer.²⁴ Recently, we have reported that mocetinostat augments the activity of docetaxel to induce apoptosis. Mocetinostat upregulates miR-31, decreases the antiapoptotic protein E2F6, and induces apoptosis in prostate cancer cells and prostate cancer stem cells.²⁵

Herein, we report a polymersome-based, PSMA-targeted, delivery system for prostate cancer, encapsulating either docetaxel or mocetinostat. We employed two FDA-approved polymers to prepare the polymersomes: PEG as the hydrophilic block and polylactic acid (PLA) as the hydrophobic block. We connected the two polymer blocks, employing the reduction-sensitive disulfide linker. We observed that the targeted polymersomes are recognized by the PSMA receptor and internalized in the prostate cancer cells LNCaP. Subsequently, the intracellular environment reductively cleaves the disulfide bond, disturbs the polymersome bilayer structure, and efficiently releases the encapsulated drugs. We observed that the combination of the two drug-encapsulated, PSMA-targeted polymersome formulations significantly ($p < 0.05$) decreased

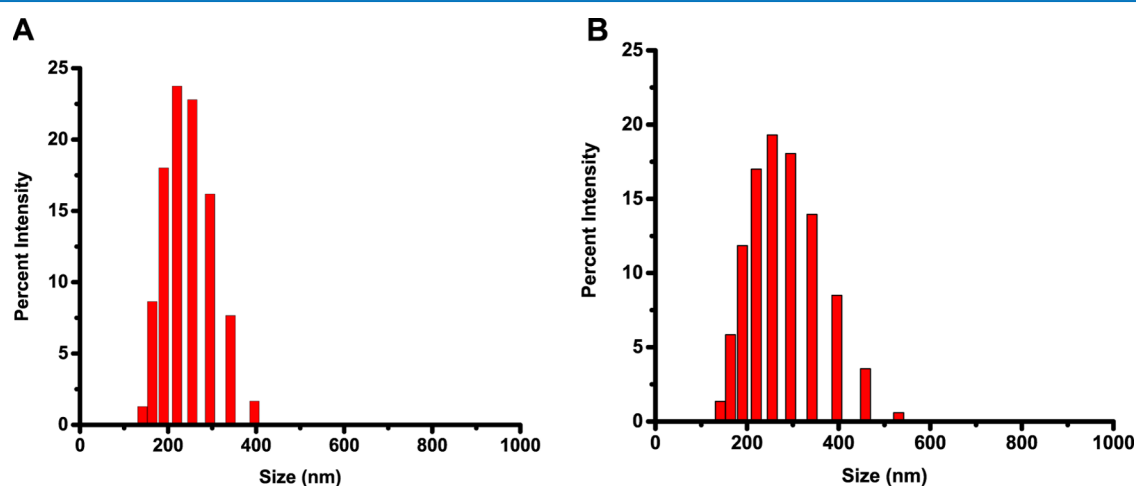


Figure 2. Size distribution of the polymersomes determined by DLS. (A) PSMA-targeted polymersomes encapsulating docetaxel; (B) PSMA-targeted polymersomes encapsulating mocetinostat.

the viability of the LNCaP cells (compared to free drugs or control) in three-dimensional (3D) spheroid cultures.

2. RESULTS AND DISCUSSION

2.1. Synthesis of the Block Copolymer and Formation of Polymersomes. To form the polymersomes, we synthesized amphiphilic block copolymers with a hydrophilic fraction (f) of 25%. We have previously demonstrated that 25% is the optimal amount of the hydrophilic polymer for forming bilayer vesicles.²⁶ The reduction-sensitive polymer PEG₂₀₀₀-SS-PLA₂₀₀₀ (Figure 1) was synthesized as reported previously.²⁶ We estimated the molecular weight of the synthesized polymer employing ¹H NMR spectroscopy. We expected the disulfide bond to cleave in the reducing microenvironment of the cell cytosol.

2.1.1. Preparation of Polymersomes. Polymersomes were prepared by the solvent-exchange method.²⁷ We incorporated 5 mol % of the DSPE-PEG₂₀₀₀-folate lipid into the polymersomes to target them to the PSMA. PSMA is highly expressed in

prostate cancer cells and hydrolyzes folate.^{15,19} The size distribution and polydispersity index of the prepared polymersomes were evaluated by dynamic light scattering (DLS) (Table 1 and Figure 2). The morphology of polymersomes was characterized by transmission electron microscopy (TEM) and atomic force microscopy (AFM) (Figures 3 and 4). We observed that the polymersomes incorporating the folate lipid were slightly larger in size (238 ± 2 nm) compared to the vesicles without the lipid (216 ± 4 nm, Table 1). Encapsulation of mocetinostat and docetaxel in the PSMA-targeted polymersomes increased the size of the nanovesicles, likely due to the accumulation of the drugs in the bilayer. The encapsulation efficiencies for mocetinostat and docetaxel were 80 and 44%, respectively. For ease of visualization, we incorporated 1 mol% of the fluorescent LR lipid into the bilayer of the polymersomes encapsulating mocetinostat. We encapsulated a small amount of the dye carboxyfluorescein in the docetaxel-encapsulated vesicles.

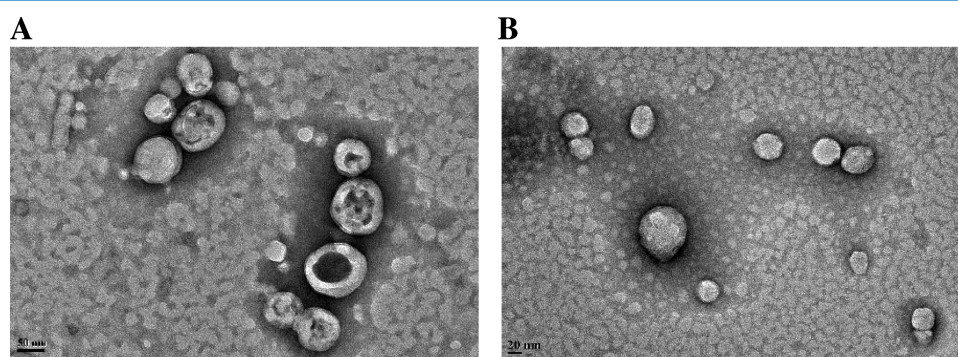


Figure 3. TEM images. (A) Polymersomes encapsulating docetaxel (scale bar is 50 nm). (B) Polymersomes encapsulating mocetinostat (scale bar is 20 nm).

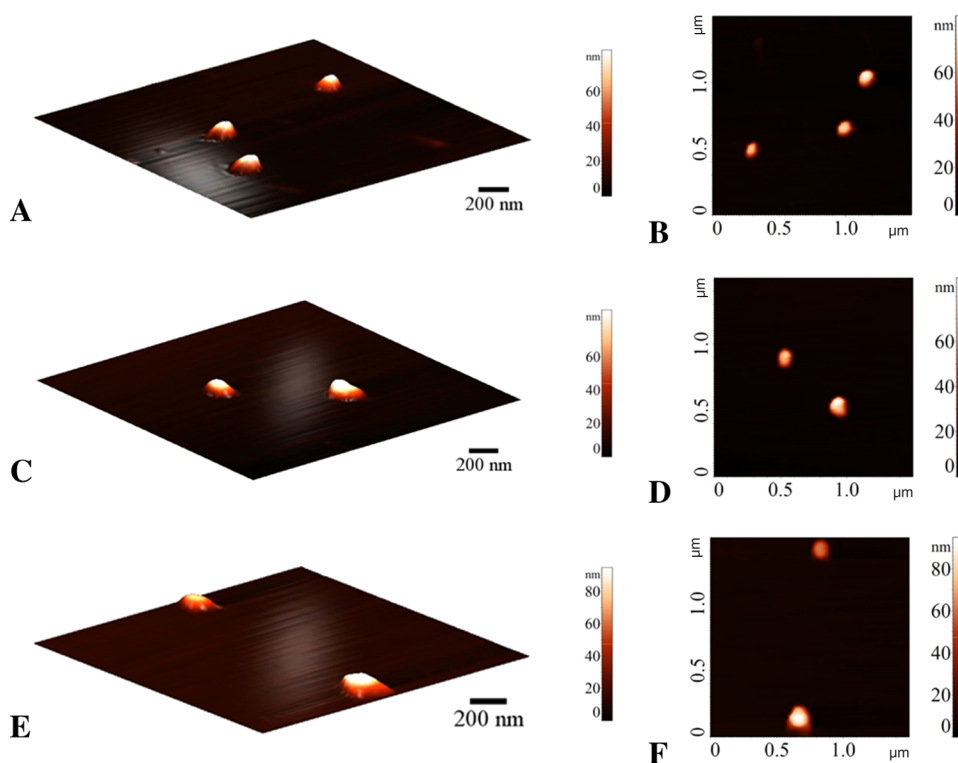


Figure 4. Atomic force microscopy (AFM) images of the polymersomes. (A, B) Polymersomes, (C, D) PSMA-targeted polymersomes encapsulating mocetinostat, and (E, F) PSMA-targeted polymersomes encapsulating docetaxel.

2.2. Demonstration of Triggered Contents Release from the Polymersomes. We encapsulated mocetinostat in the polymersomes and monitored the reduction-triggered release of the drug as a function of time with different concentrations of added glutathione (GSH). GSH is a tripeptide

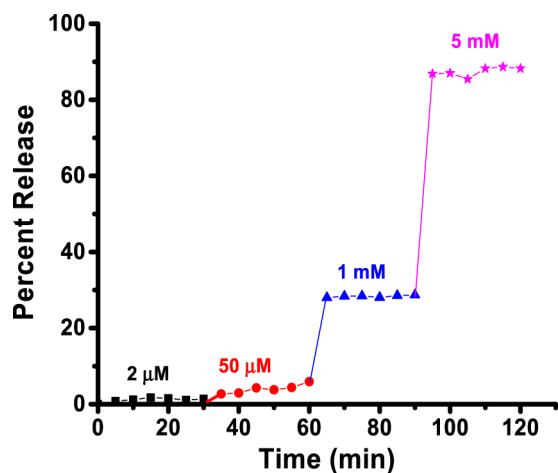


Figure 5. Reduction-mediated release profile of encapsulated mocetinostat from the polymersomes. The drug-encapsulated vesicles were treated with 2 μM (black squares), 50 μM (red circles), 1 mM (blue triangles), and 5 mM (pink stars) of GSH. The lines connecting the data points are also shown.

consisting of glutamic acid, cysteine, and glycine. The majority of GSH (90%) is available in the cytosol, and its increased level is correlated with progression and proliferation of cancerous cells.²⁸ Treatment with circulation levels of glutathione (2 μM) released less than 1% of the drug in 30 min (Figure 5, black

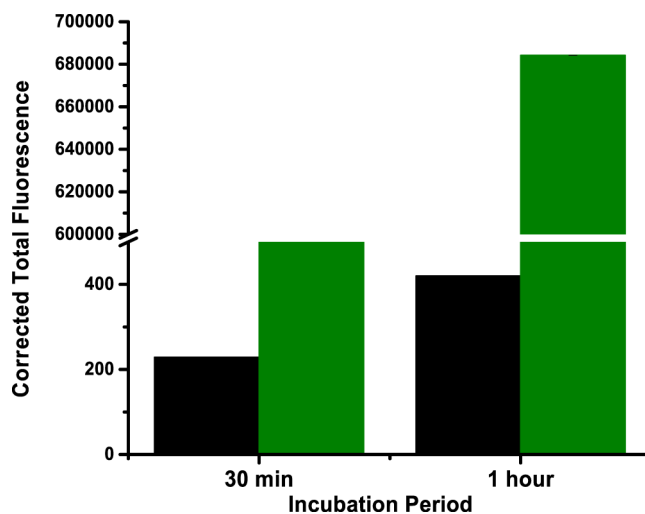


Figure 7. CTCF analysis of the images of the LNCaP cells incubated with the PSMA-targeted polymersomes (green bars) and the non-targeted polymersomes (black bars).

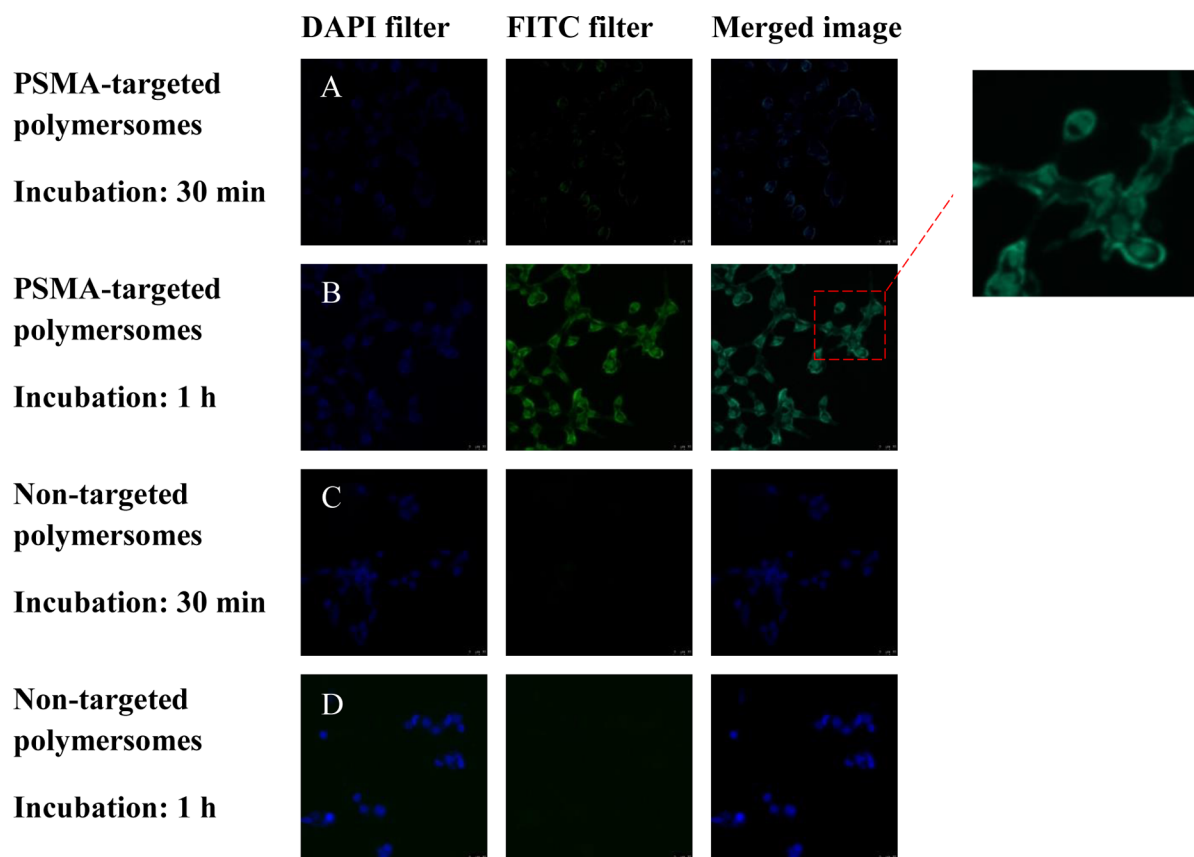


Figure 6. Fluorescence microscopic images of LNCaP cell incubated with the polymersomes (magnification: 20 \times). The nuclei of the cells were stained with the Hoechst dye (blue image, 4',6-diamidino-2-phenylindole filter). The polymersome images are green due to the encapsulated carboxyfluorescein (fluorescein isothiocyanate filter). The merged images are shown in the third panel. (A) PSMA-targeted polymersomes after 30 min incubation, (B) PSMA-targeted polymersomes after 1 h incubation, (C) nontargeted polymersomes after 30 min incubation, and (D) nontargeted polymersomes after 1 h incubation.

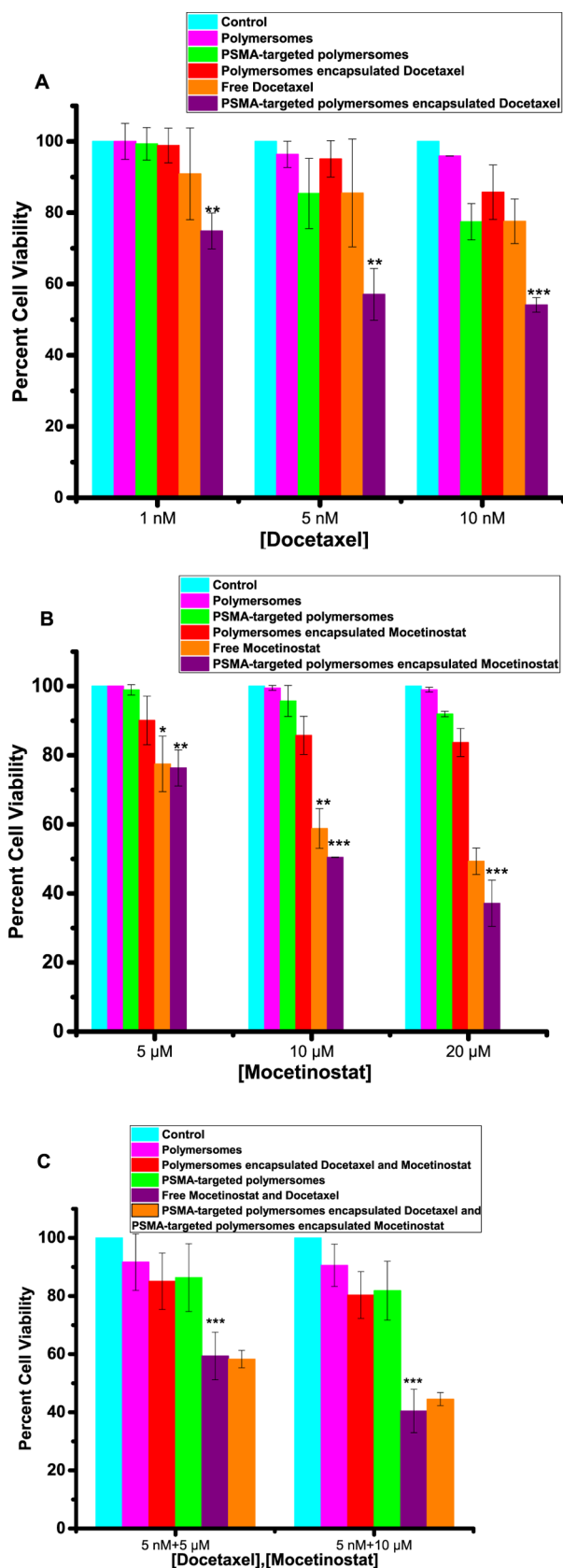


Figure 8. Viability of the LNCaP cells in monolayer cultures. (A) Cell viability with media only (control, cyan bar), nontargeted polymersomes (pink bar), nontargeted polymersomes encapsulating docetaxel (red bar), targeted polymersomes (green bar), free docetaxel (orange bar), and targeted polymersomes encapsulating docetaxel (purple bar). (B) Cell viability with media only (control, cyan bar), nontargeted

Figure 8. continued

polymersomes (pink bar), nontargeted polymersomes encapsulating mocetinostat (red bar), targeted polymersomes (green bar), free docetaxel (orange bar), and targeted polymersomes encapsulating mocetinostat (purple bar). (C) Cell viability with media only (control, cyan bar), nontargeted polymersomes (pink bar), nontargeted polymersomes encapsulating docetaxel/mocetinostat (red bar), targeted polymersomes (green bar), free docetaxel and mocetinostat (orange bar), and the combination of targeted polymersomes encapsulating docetaxel/mocetinostat (purple bar). The data presented are representative of three individual experiments. Error bars denote the mean \pm SEM. Statistical analysis: Student's *t*-test where * $p < 0.05$, ** $p < 0.001$, and *** $p < 0.0001$.

squares). We increased the concentration of GSH to match the extracellular matrix level (50 μ M) and observed 10% release of encapsulated mocetinostat (Figure 6, red circles). The cytosolic concentration of glutathione (1–5 mM) led to substantial release (30–85%) of the encapsulated drug from the polymersomes (Figure 5, blue triangles and magenta stars). Because of the very low amount of docetaxel encapsulated in the polymersomes (nanomolar concentration), we did not study the release profile from these vesicles in the presence of varying concentrations of added reducing agents.

2.3. Uptake of the Polymersomes in Monolayer Culture of Prostate Cancer Cells. To demonstrate cytosolic localization in the prostate cancer cells, we prepared polymersomes incorporating 5% DSPE-PEG₂₀₀₀-folate into the bilayer. The LNCaP prostate cancer cells overexpress the PSMA receptor on the surface.²⁹ We incubated the cultured LNCaP cells with PSMA-targeted and nontargeted polymersomes (encapsulating carboxyfluorescein) for different times, washed the cells, and imaged them employing a fluorescence microscope (Figure 6). We observed higher localization of the targeted polymersomes after 1 h of incubation with the LNCaP cells. We analyzed the images employing the Image J software. The corrected total cell fluorescence (CTCF) intensity clearly indicated that the targeted polymersomes internalized more in the LNCaP cells compared to the nontargeted vesicles (Figure 7).

After demonstrating efficient cellular internalization, we proceeded to determine the effectiveness of the PSMA-targeted drug-encapsulated polymersomes. We investigated the effect of targeted polymersomes on both PSMA-positive (LNCaP) and PSMA-negative (PC3) prostate cancer cell lines. The cultured LNCaP and PC3 cells were treated with the polymersome formulations encapsulating mocetinostat or docetaxel and the free drugs for 48 h. Subsequently, the cell viability was examined by the Alamar Blue assay because the reagents used for this assay do not interact with nanoparticles.³⁰ We observed that the PSMA-targeted polymersomes encapsulating mocetinostat (or docetaxel) significantly reduced ($p \leq 0.001$) the cell viability compared to the control (medium only) for the LNCaP cells. We also observed dose-dependent cellular toxicity for the drug-encapsulated polymersomes (Figure 8). As the concentration is increased, the PSMA-targeted, drug-encapsulated polymersomes showed higher toxicity to the LNCaP cells. For example, with 10 nM encapsulated docetaxel, the viability of the LNCaP cells decreased to 54% (Figure 8B). Interestingly, we also observed much less cellular toxicity in the PC3 cells, suggesting that the PSMA-targeted polymersomes encapsulating mocetinostat/docetaxel can internalize through the PSMA receptor on the LNCaP cells (Figure 9). Literature reports indicate that the PC3 cells express a small amount of PSMA receptors on the surface, and

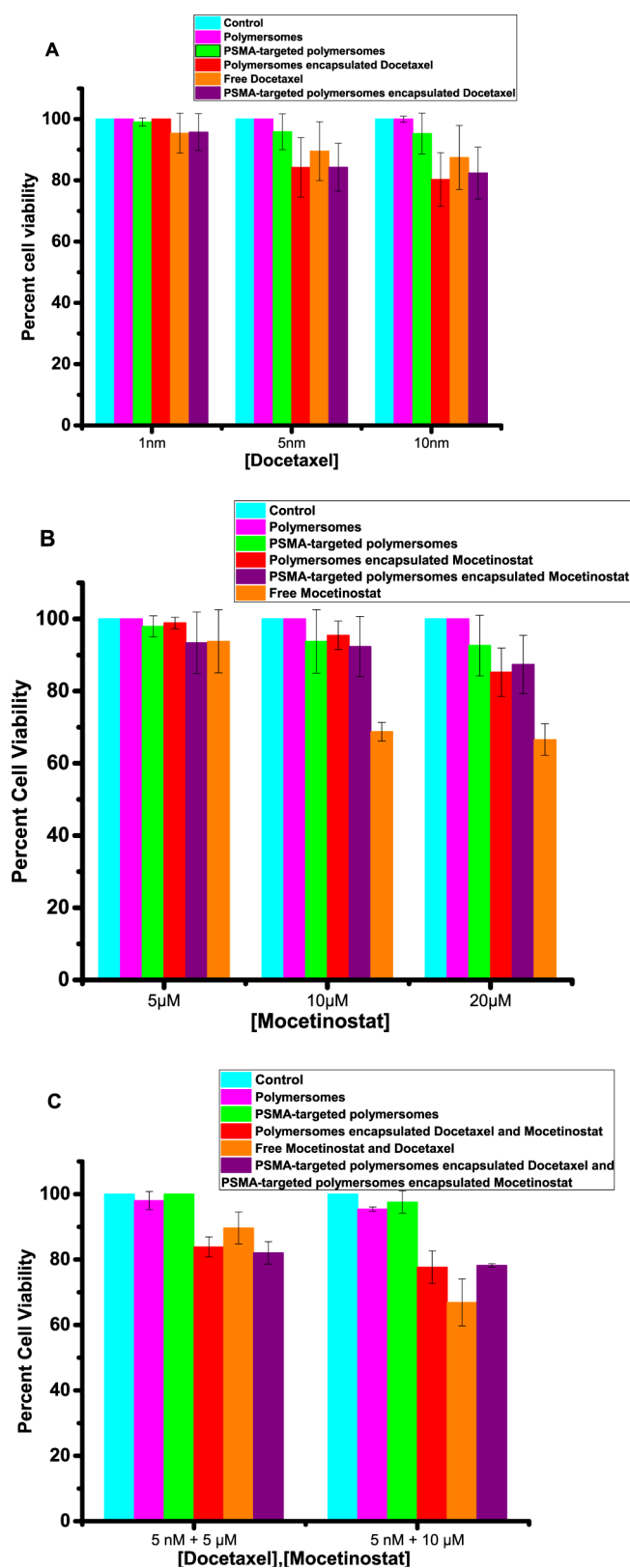


Figure 9. Viability of the PC3 cells in monolayer cultures. (A) Cell viability with media only (control, cyan bar), nontargeted polymersomes (pink bar), targeted polymersomes (green bar), nontargeted polymersomes encapsulating docetaxel (red bar), free docetaxel (orange bar), and targeted polymersomes encapsulating docetaxel (purple bar). (B) Cell viability with media only (control, cyan bar), nontargeted polymersomes (pink bar), targeted polymersomes (green bar), nontargeted polymersomes encapsulating mocetinostat (red bar), free docetaxel and mocetinostat (orange bar), and the combination of targeted polymersomes encapsulating docetaxel/mocetinostat (purple bar). Error bars denote the mean \pm SEM.

Figure 9. continued

docetaxel (orange bar), and targeted polymersomes encapsulating mocetinostat (purple bar). (C) Cell viability with media only (control, cyan bar), nontargeted polymersomes (pink bar), targeted polymersomes (green bar), nontargeted polymersomes encapsulating docetaxel/mocetinostat (red bar), free docetaxel and mocetinostat (orange bar), and the combination of targeted polymersomes encapsulating docetaxel/mocetinostat (purple bar). Error bars denote the mean \pm SEM.

the expression level is upregulated by the basic fibroblast growth factor.¹⁷

After demonstrating the effects of the PSMA-targeted drug-encapsulated polymersomes, we proceeded to determine the synergistic effect of the two formulations encapsulating mocetinostat and docetaxel. The cells were treated with the combination of docetaxel- and mocetinostat-encapsulated vesicles as well as the appropriate controls. The results revealed significant ($p \leq 0.0001$) cytotoxicity for the combination formulation (5 nM docetaxel + 10 μ M mocetinostat) compared to the controls for the LNCaP cells (Figure 8C). However, we observed that the cell viability of the combination formulation was similar to that of the mixture of the two free drugs (Figure 8C). We note that the drug-encapsulated polymersomes will be advantageous due to the passive targeting of the vesicles by the EPR effect and the resultant reduced systemic toxicity. To determine any synergistic effects in the LNCaP cells, we calculated the combination index (CI) for combining the targeted polymersomes encapsulating mocetinostat and the targeted polymersomes encapsulating docetaxel employing the CalcuSyn software (www.biosoft.com). The CI values indicated that the combination formulation is synergistically reducing the viability of the LNCaP cells (Table 2). The drug-encapsulated polymersomes were significantly less toxic to the PC3 cells compared to the LNCaP cells. We did not observe enhanced cellular toxicity of the combination of the two drug-encapsulated polymersomes in the PC3 cells (Figure 9). Co-administration of PSMA-targeted polymersomes encapsulating mocetinostat and docetaxel significantly decreased the viability of the LNCaP cells ($p < 0.05$) compared to the PC3 cells in monolayer cultures.

2.4. Cytotoxicity in the 3D Spheroid Cultures.

Monolayer cell cultures do not adequately model prostate cancer due to the lack of cell–cell and cell–matrix interactions.³¹ In contrast to the monolayer cultures, the 3D spheroids have intercellular interactions, the necrotic cores, and the heterogeneity that mimics the in vivo tumors.³² To demonstrate the usefulness of our approach, we have tested the polymersomes on cultured uniform-sized 3D spheroids of the LNCaP and PC3 cells. We prepared the spheroids using an agar mold, and after growing them for 10 days, we incubated them with the polymersomes and free drugs. On the basis of the results from the monolayer cultures of the LNCaP cells, we used 5 nM docetaxel and 10 mM mocetinostat (either free or polymersome-

Table 2. Calculated CI for the Combination of Targeted Polymersomes Encapsulating Mocetinostat and the Targeted Polymersomes Encapsulating Docetaxel in the LNCaP Cells

[mocetinostat] (μ M)	[docetaxel] (nM)	CI
5	2	0.45
10	4	0.29
20	8	0.19

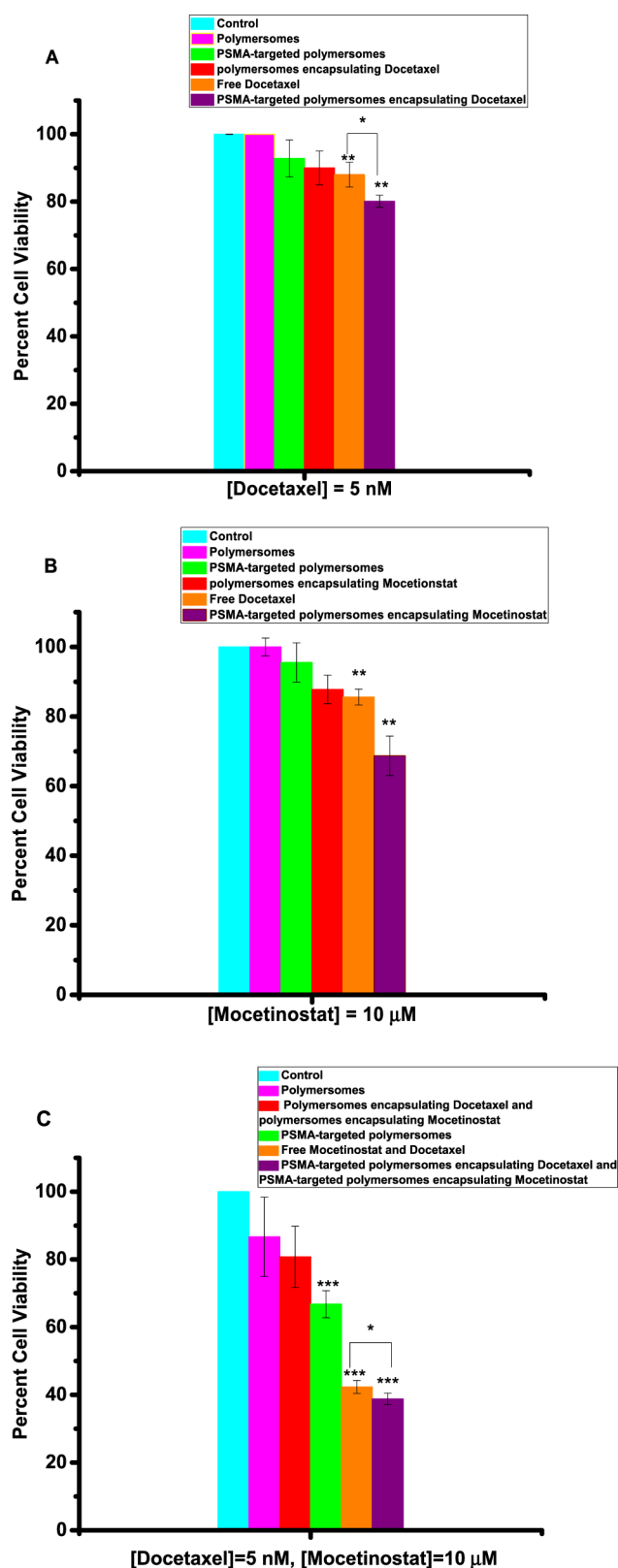


Figure 10. Viability of LNCaP cells in 3D spheroid cultures. (A) Docetaxel-encapsulated, targeted polymersomes (purple bar) were more potent compared to the free drug (orange bar), targeted vesicles without any drug (green bar), nontargeted polymersomes without any drug (pink bar), and the media (cyan bar). (B) Mocetinostat-encapsulated, targeted polymersomes (purple bar) were more potent compared to the free drug (orange bar), targeted vesicles without any drug (green bar), nontargeted polymersomes without any drug (pink

Figure 10. continued

bar), and the media (cyan bar). (C) The combination of docetaxel/mocetinostat-encapsulated targeted polymersomes (purple bar) was more potent compared to the free drug (orange bar), targeted vesicles without any drug (green bar), nontargeted polymersomes without any drug (pink bar), and the media (cyan bar). Data presented are representative of three individual experiments. Error bars denote the mean \pm SEM. Statistical analysis: Student's *t*-test where * $p < 0.05$, ** $p < 0.001$, and *** $p < 0.0001$.

encapsulated) in the spheroids of the LNCaP and PC3 cells. We observed enhanced cytotoxicity (by the Alamar Blue assay) for the polymersome-encapsulated mocetinostat (or docetaxel) compared to the control or the unencapsulated drugs (Figure 10A,B). We also observed that the combination of the two drug-encapsulated polymersomes was more potent compared to either mocetinostat or docetaxel (free or encapsulated in the vesicles, Figure 10C). The combination decreased the cell viability to 39% in the LNCaP spheroids (Figure 10C, purple bar). The effect of the drug-encapsulated polymersomes was significantly less in the spheroids of the PC3 cells (Figure 11) compared to the LNCaP cells ($p < 0.001$).

To determine the penetration depth and the effect of the drug-encapsulated polymersomes, we sliced (160 μm thick) the treated, LNCaP cell spheroids using a microtome (Figure 12). We imaged the spheroid slices using a commercially available live–dead cell imaging kit. The live cells hydrolyze the calcein-AM dye to calcein (green fluorescence).³³ Ethidium homodimer-1 passes through the membranes of damaged cells, binds to the DNA, and emits a red fluorescence.³³ We observed that co-treatment of the spheroids with mocetinostat- and docetaxel-encapsulated, targeted polymersomes leads to primarily dead cells (Figure 13A,B). The cells in the control spheroids (without any treatment) were alive, producing the green fluorescence (Figure 13C,D). The CTCF was calculated using software Image J (Figures 13 and 14). The analysis indicated that the control spheroid slices contain primarily live cells, whereas the treated slices have mainly the dead cells.

3. EXPERIMENTAL SECTION

PEG–S–S–PLA was synthesized by ring-opening polymerization as previously reported from our laboratory.²⁶ Briefly, PEG (MW:2000) was reacted with succinic anhydride and then conjugated to cystamine dihydrochloride in the presence of EDC. The PLA polymer was subsequently synthesized from D-,L-lactide and a catalytic quantity of octyl tin (II).

3.1. Preparation and Characterization of Polymersomes. The polymersomes were prepared by the solvent-exchange method¹³ using the synthesized PEG₂₀₀₀–SS–PLA₆₂₀₀ and the commercially available fluorescent lissamine rhodamine lipid [LR; 1,2-dipalmitoyl-*sn*-glycero-3-phosphoethanolamine-*N*-(lissamine rhodamine B sulfonyl) (ammonium salt)] in molar proportions of 95:5, respectively. The LR lipid was dissolved in chloroform (0.01 mg/mL). The polymer (0.9% w/v) was dissolved in tetrahydrofuran (THF). The chloroform was removed using a rotary evaporator to prepare a thin film. The polymer solution was added slowly to the thin film, and then the mixture was added dropwise to a stirred 10 mM *N*-(2-hydroxyethyl)piperazine-*N'*-ethanesulfonic acid (HEPES) buffer (pH 7.4). Polymersome solutions were stirred for 45 min at room temperature, and then air was passed for 45 min through the mixture to remove the organic solvent. The formed

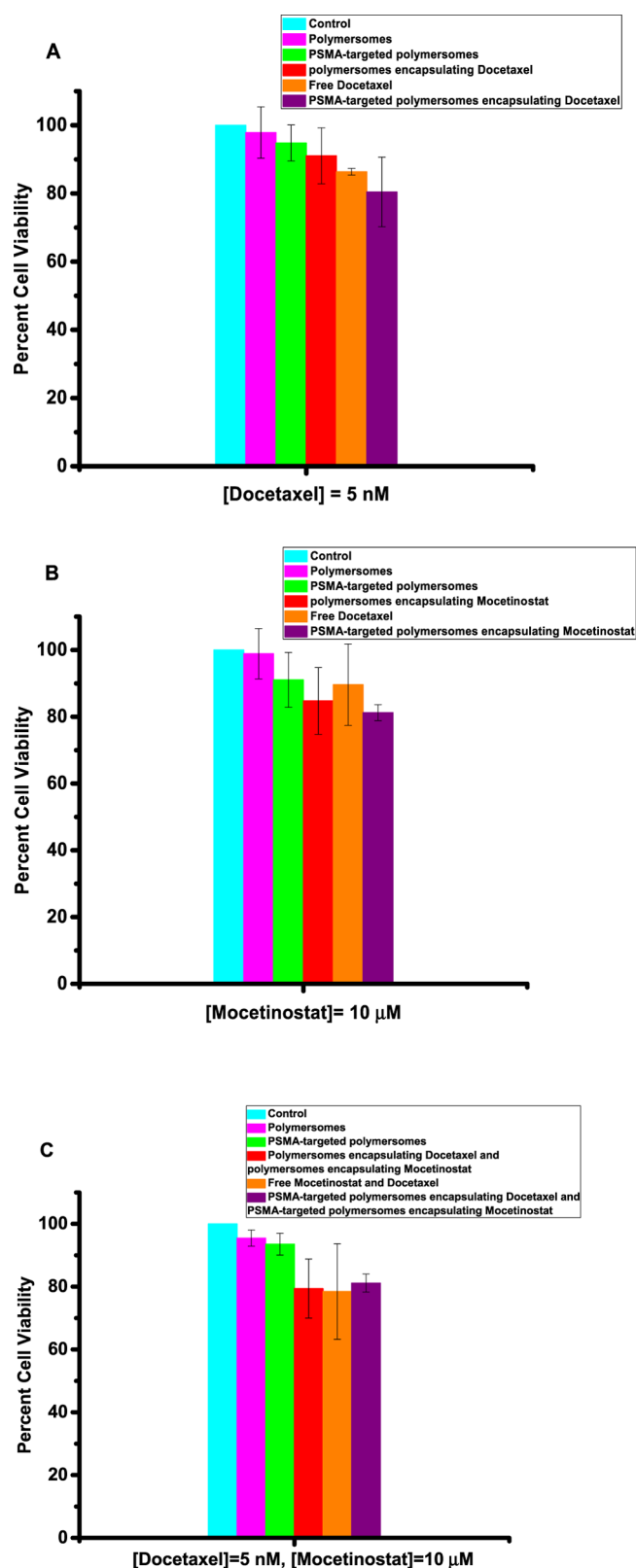


Figure 11. Viability of PC3 cells in 3D spheroid cultures. (A) Docetaxel-encapsulated targeted polymersomes (purple bar) were more potent compared to the free drug (orange bar), targeted vesicles without any drug (green bar), nontargeted polymersomes encapsulating docetaxel (red bar), nontargeted polymersomes without any drug (pink bar), and the media (cyan bar). (B) Mocetinostat-encapsulated, targeted polymersomes (purple bar) were more potent compared to the free drug (orange bar), targeted vesicles without any drug (green bar),

Figure 11. continued

nontargeted polymersomes encapsulating mocetinostat (red bar), nontargeted polymersomes without any drug (pink bar), and the media (cyan bar). (C) Combination of docetaxel/mocetinostat-encapsulated, targeted polymersomes (purple bar) was as potent as the free drug (orange bar) and nontargeted polymersomes encapsulating docetaxel/mocetinostat (red bar), targeted vesicles without any drug (green bar), nontargeted polymersomes without any drug (pink bar), and the media (cyan bar). Data presented are representative of three individual experiments. Error bars denote the mean \pm SEM. Statistical analysis: Student's *t*-test where **p* < 0.05, ***p* < 0.001, and ****p* < 0.0001.

polymersomes were sonicated at 25 °C for 70 min (Symphony 117 V, 60 Hz). Subsequently, the polymersomes were passed through a Sephadex G100 (GE Healthcare) size-exclusion column to collect dye-encapsulated polymersomes. These polymersomes were used for the cell viability assays.

3.2. Preparation of Polymersomes Encapsulating Mocetinostat or Docetaxel (with and without PSMA Targeting).

The nanovesicles were prepared using the PEG₁₉₀₀-SS-PLA₆₀₀₀ polymer, DSPE-PEG₂₀₀₀-folate lipid, and LR lipid in molar proportions of 95:5:5, respectively. Mocetinostat and docetaxel were encapsulated into the polymersomes by the solvent-exchange method.²⁷ The nontargeted polymersomes encapsulating mocetinostat or docetaxel were prepared the same way without using the DSPE-PEG₂₀₀₀-folate lipid. Briefly, the polymer and the lipid were dissolved in chloroform. Mocetinostat and docetaxel (0.125% w/v) were dissolved in THF. The two drugs were added to the polymer solutions in two different vials and slowly added to the solution of folate-conjugated lipid in two different vials. For the ease of visualization, the LR lipid was incorporated into the polymersomes encapsulating mocetinostat, and carboxyfluorescein (100 μM) was encapsulated along with docetaxel in the other formulation. The resultant solutions were added dropwise to stirred HEPES buffer (10 mM, pH 7.4). Polymersomes were stirred for 45 min, and then air was passed through drug-loaded nanovesicles for another 45 min. The nanovesicles were sonicated at 25 °C for 70 min (Symphony 117 V, 60 Hz). The polymersomes (1 mg/mL) were passed through the Sephadex G100 size-exclusion column to remove the unencapsulated drug.

Drug-loading efficiencies (DLE) of the polymersomes were determined using UV-vis spectroscopy. After passing through the size-exclusion column, the absorption of the polymersomes was recorded at 230 nm. The calibration curves were generated for each drug separately. The DLE for mocetinostat and docetaxel were determined according to the following equation

$$\text{DLE \%} = \frac{\text{mass of drug loaded into polymersomes}}{\text{total drug added}} \times 100$$

3.3. Size-Distribution Analysis. The size distributions of the polymersomes were determined by the DLS method, employing the NanoZS 90 Zetasizer (Malvern Instruments). The measurements were conducted in disposable polystyrene cuvettes at a scattering angle of 90° (polymersome concentration: 1 mg/mL). The samples were equilibrated for 2 min; five repeats were recorded with 10 measurements for each sample.

3.4. TEM. Copper TEM grids (300-mesh, formvar-carbon coated, Electron Microscopy Sciences, Hatfield, Pennsylvania) were prepared by applying a drop of 0.01% poly-L-lysine, allowing it to stand for 30 s, wicking off the liquid with torn filter

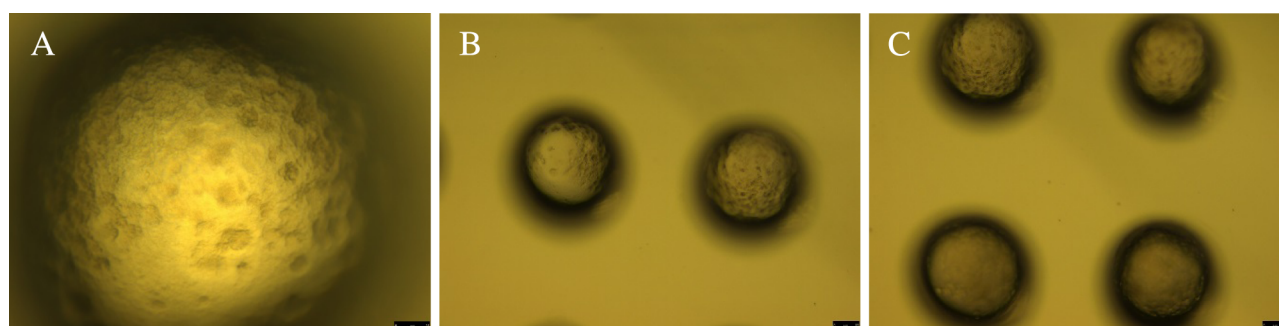


Figure 12. Optical images of the slices from the 3D spheroids of LNCaP cells (scale bars: $25\ \mu\text{m}$). Bright field images of the LNCaP cell spheroids in $20\times$ (A), $10\times$ (B), and $4\times$ (C) magnifications. The 3D spheroids were treated with the combination of PSMA-targeted polymersomes encapsulating docetaxel ($5\ \text{nM}$)/mocetinostat ($10\ \mu\text{M}$).

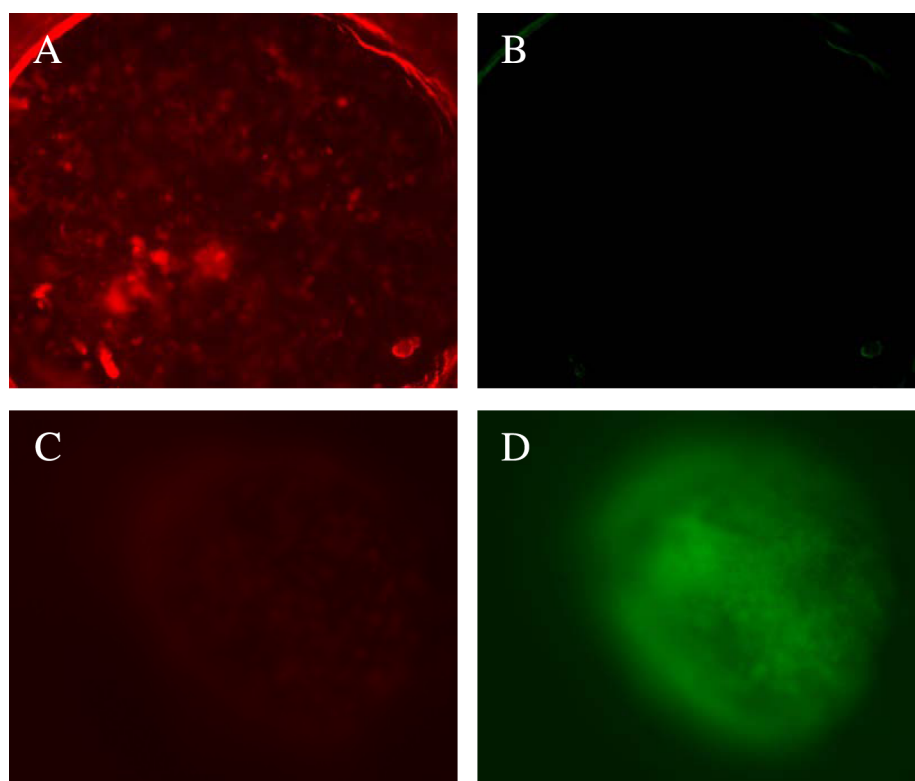


Figure 13. Live–dead cell assays for slices of LNCaP cell spheroids. Treatment of the LNCaP spheroids with mocetinostat ($10\ \mu\text{M}$)- and docetaxel ($5\ \text{nM}$)-encapsulated, targeted polymersomes produces primarily dead cells (A) with very few live cells (B). The Control sample showed a few dead cells (C) and mainly live cells (D).

paper, and allowing the grids to air dry. A drop of the polymersomes was placed on the prepared grid for 30 s and wicked off; grids were allowed to air dry again. Phosphotungstic acid 0.1%, pH adjusted to 7–8, was dropped onto the grid containing the sample, allowed to stand for 2 min, and wicked off. After the grids were dry, images were obtained using a JEOL JEM-2100 LaB6 transmission electron microscope (JEOL USA, Peabody, Massachusetts) running at 200 keV.

3.5. AFM. Polymersomes ($0.5\ \text{mg/mL}$) were diluted ($10\times$) in 10 mM HEPES buffer (pH 7.4), dropped on silica substrates, and incubated for a minute and subjected to an air blow gun. The AFM measurements were conducted in noncontact mode at a resonance frequency of 145 kHz and scanning rate of 1.3 Hz and using an NT-MDT INTEGRA (NT-MDT America). The scanning areas were $5 \times 5\ \mu\text{m}^2$ at a resolution of 512 points per line.

3.6. Redox-Triggered Release Study. The release of mocetinostat from the PSMA-targeted polymersomes was monitored in the presence of glutathione (GSH). Polymersomes loaded with the drug ($500\ \mu\text{L}$ of $1\ \text{mg/mL}$ solution) were dispensed into a dialysis tube (Spectra/Por Float-A-LyzerG2 Dialysis Tubes, MWCO: 500–1000 Da, diameter: 10 mm, volume: 1 mL). GSH was added after 5 min, and the concentration of GSH was increased every 30 min. The GSH concentrations were $2\ \mu\text{M}$ (circulation levels of glutathione),³⁴ $50\ \mu\text{M}$ (extracellular matrix level),²⁶ $1\ \text{mM}$, and $5\ \text{mM}$ (cytosolic concentration of glutathione)²⁶ after the successive addition steps. The absorbance of the aqueous solution (at 230 nm) from the outside tube was measured every 5 min using a UV spectrophotometer (Spectramax M5, Molecular Devices). Subsequently, the percent release was calculated from the calibration curve.

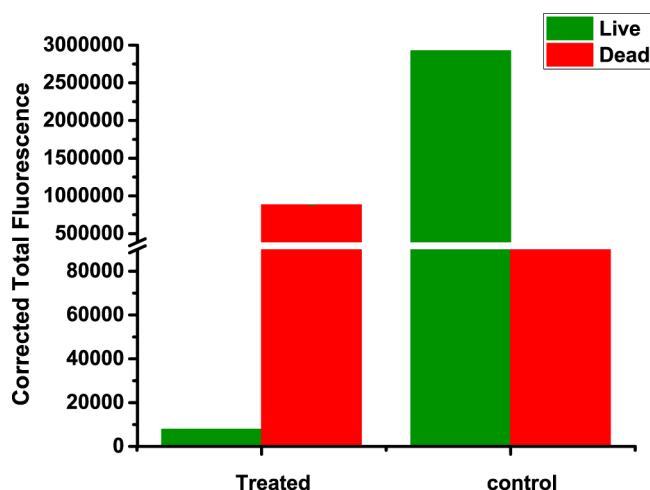


Figure 14. CTCF analysis of the spheroid slices after the live–dead assay. The LNCaP spheroids were treated with mocetinostat (10 μ M)- and docetaxel (5 nM)-encapsulated PSMA-targeted polymersomes. The green bars indicate the intensity of images for the live cells, and the red bars indicate the intensity of the images for the dead cells.

3.7. Culture of Human Prostate Carcinoma Cells. The prostate cancer cell lines LNCaP and PC3 were purchased from American Type Culture Collection. The cells were maintained in RPMI 1640 medium (without phenol red), supplemented with 1% v/v antibiotics (penicillin and streptomycin), 10% v/v fetal bovine serum, and 2.05 mM L-glutamate. The cell culture flasks were incubated at 37 °C in a 5% CO₂ atmosphere.

3.8. Cellular Uptake of PSMA-Targeted Polymersomes. The cultured LNCaP cells (3×10^3) were seeded in an uncoated 8-well glass bottom plate for 24 hours before the experiment. When 90% confluent, the PSMA-targeted (20 μ L) and the control polymersomes (20 μ L) encapsulating carboxyfluorescein were incubated with the cells for 30 min. Subsequently, the media were removed, and the cells were washed thrice with Hanks' balanced salt solution (HBSS) to remove the non-internalized polymersomes. Subsequently, the cell nuclei were stained with HOESCHT 33342 dye (Enzo Life Sciences, 1/1000 dilution) and imaged employing a fluorescence microscope. The same experiment was repeated with 1 h incubation time with the polymersomes.

3.9. Cytotoxicity Studies in Monolayer Cell Cultures. The Alamar Blue assay was conducted to evaluate the viability of the human prostate carcinoma cells. The LNCaP and PC3 cells were seeded at a density of $1 \times 10^3/200 \mu$ L in a 96-well tissue culture plate before the experiment and were allowed to grow until 80–95% confluent. The plate was divided into six groups: control, free drugs, nontargeted polymersomes, nontargeted polymersomes encapsulating drugs, PSMA-targeted polymersomes, and PSMA-targeted polymersomes encapsulating the drugs. Separately, similar experiments were conducted for mocetinostat and docetaxel. The control group did not receive any treatment. Cells treated with mocetinostat formulations received 5, 10, and 20 μ M of free and an equivalent amount of encapsulated drug. The docetaxel treatment group received 1, 5, and 10 nM of free drug, and the docetaxel-encapsulated polymersomes containing the same amounts of the drug. The cells were treated with the free or encapsulated drugs for 48 h at 37 °C, in a 5% CO₂ atmosphere. Subsequently, the cells were washed thrice with sterile HBSS and replaced with 200 μ L fresh media. The cell viability was determined using the Alamar Blue

assay following the manufacturer's protocol. Subsequently, we evaluated the effects of the combination of both drug formulations on the treated cells using the same protocol. The data presented are normalized to the control.

3.10. Cytotoxicity Studies in a 3D Spheroid Cell Culture. The LNCaP and PC3 cell spheroids were prepared by using 96-well 3D Petri Dishes (Microtissues). Briefly, 2% w/v agarose solution in water was prepared and autoclaved. The cell suspension (1×10^4 cell/60 μ L media) was added to each 3D scaffold. The cells were allowed to grow for 10 days to form the spheroids. The scaffold was then divided into six groups: control, nontargeted polymersomes, nontargeted polymersomes encapsulating drugs, targeted polymersomes, targeted polymersomes encapsulating mocetinostat or docetaxel. The spheroids were treated for 48 h with the same concentration of drugs as used for the monolayer studies. Subsequently, the excess medium was removed, and the spheroids were incubated with TryPLE (recombinant trypsin, Life Technologies, 100 μ L) for 10 min. The dislodged spheroids were removed and subjected to the Alamar Blue assay. The data presented are normalized to the control.

3.11. Live–Dead Cellular Assay. The LNCaP spheroids were prepared as described in the previous section. The live–dead cellular assays were performed on the spheroids treated with a combination of mocetinostat-encapsulated and docetaxel-encapsulated PSMA-targeted polymersomes, PSMA-targeted polymersomes, polymersomes, free drugs, and control. After the treatment and washing, 160 μ m thick slices of the spheroids were prepared using microtome HM 355 S. A commercially available live–dead assay kit (Calcein-AM/Ethidium homodimer-1, Biotium) for mammalian cells was used to image the live and dead cells in each of the slices. We analyzed the images employing the Image J software. We selected three random regions and calculated the CTCF using the formula

$$\text{CTCF} = \text{integrated density} - (\text{area of selected cell} \\ \times \text{mean fluorescence of background readings})$$

4. CONCLUSIONS

We have prepared polymersomes from the synthesized, amphiphilic polymers containing PEG as the hydrophilic block. We have successfully demonstrated that the PSMA can be used to target the polymersomes actively to prostate cancer cells. After internalization, the large amount of reducing agent in the cytosol triggers the release of encapsulated hydrophobic drugs from the polymersomes. A combination of PSMA-targeted vesicles encapsulating mocetinostat and docetaxel reduced the viability of LNCaP prostate cancer cells (expressing the PSMA receptor) in 3D spheroid cultures. The CI value (CI < 1) indicated that the combination of mocetinostat and docetaxel-encapsulated polymersomes had a synergistic effect in reducing the viability of the prostate cancer cells. Our imaging analysis confirmed that the combination of the two drug-encapsulated polymersomes primarily kills the cancer cells. We expect that our results will motivate further research into stimuli-responsive, targeted polymersomes and the use of 3D cellular models for testing the cytotoxicity of drug formulations.

AUTHOR INFORMATION

Corresponding Author

*E-mail: Sanku.Mallik@ndsu.edu.

Present Addresses

^{||}Department of Pharmaceutical Sciences, University of Houston, 3455 Cullen Blvd., Houston, Texas 77204, United States (B.G.).

[§]American Radiolabeled Chemicals, Inc., 101 ARC Drive, Saint Louis, Missouri 63146, United States (M.K.H.).

Notes

The authors declare no competing financial interest.

ACKNOWLEDGMENTS

This research was supported by the NSF grant DMR 1306154 and NIH grant 1 R01GM 114080 to SM. The Electron Microscopy Center is supported by the NSF Grant MRI 0821655. We thank Ibidi Inc. and Cellvis Inc. for the gift of glass bottom plates for cellular studies. YC acknowledges support from the NDSU startup funds, the NSF EPSCoR New Faculty Award, and the ND NASA EPSCoR RID Grant.

REFERENCES

- (1) Siegel, R. L.; Miller, K. D.; Jemal, A. Cancer statistics, 2015. *Ca-Cancer J. Clin.* **2015**, *65*, 5–29.
- (2) American Cancer Society, 2016. www.cancer.org.
- (3) Li, C. Q.; Zhang, G. X. Nanosize delivery as an emerging platform for cancer therapy. *Cancer Biol. Ther.* **2008**, *7*, 1860–2.
- (4) Peer, D.; Karp, J. M.; Hong, S.; Farokhzad, O. C.; Margalit, R.; Langer, R. Nanocarriers as an emerging platform for cancer therapy. *Nat. Nanotechnol.* **2007**, *2*, 751–760.
- (5) Gao, Y.; Li, Y.; Li, Y.; Yuan, L.; Zhou, Y.; Li, J.; Zhao, L.; Zhang, C.; Li, X.; Liu, Y. PSMA-mediated endosome escape-accelerating polymeric micelles for targeted therapy of prostate cancer and the real time tracing of their intracellular trafficking. *Nanoscale* **2015**, *7*, 597–612.
- (6) Farokhzad, O. C.; Jon, S.; Khademhosseini, A.; Tran, T.-N. T.; LaVan, D. A.; Langer, R. Nanoparticle-aptamer bioconjugates a new approach for targeting prostate cancer cells. *Cancer Res.* **2004**, *64*, 7668–7672.
- (7) Kroon, J.; Buijs, J. T.; van der Horst, G.; Cheung, H.; van der Mark, M.; van Bloois, L.; Rizzo, L. Y.; Lammers, T.; Pelger, R. C.; Storm, G.; et al. Liposomal delivery of dexamethasone attenuates prostate cancer bone metastatic tumor growth in vivo. *The Prostate* **2015**, *75*, 815–824.
- (8) Katti, K. S.; Molla, M.; Karandish, F.; Haldar, M. K.; Mallik, S.; Katti, D. R. Sequential culture on biomimetic nanoclay scaffolds forms three-dimensional tumoroids. *J. Biomed. Mater. Res., Part A* **2016**, *104*, 1591–1602.
- (9) Cheng, C. J.; Saltzman, W. M. Polymer Nanoparticle-Mediated Delivery of MicroRNA Inhibition and Alternative Splicing. *Mol. Pharmaceutics* **2012**, *9*, 1481–1488.
- (10) Lewin, M.; Carlesso, N.; Tung, C.-H.; Tang, X.-W.; Cory, D.; Scadden, D. T.; Weissleder, R. Tat peptide-derivatized magnetic nanoparticles allow in vivo tracking and recovery of progenitor cells. *Nat. Biotechnol.* **2000**, *18*, 410–414.
- (11) Liu, X.; Liu, C.; Laurini, E.; Posocco, P.; Pricl, S.; Qu, F.; Rocchi, P.; Peng, L. Efficient delivery of sticky siRNA and potent gene silencing in a prostate cancer model using a generation 5 triethanolamine-core PAMAM dendrimer. *Mol. Pharmaceutics* **2012**, *9*, 470–81.
- (12) Katti, K. S.; Molla, M.; Karandish, F.; Haldar, M. K.; Mallik, S.; Katti, D. R. Sequential culture on biomimetic nanoclay scaffolds forms three-dimensional tumoroids. *J. Biomed. Mater. Res., Part A* **2016**, *104*, 1591–1602.
- (13) Lee, J. S.; Feijen, J. Polymersomes for drug delivery: Design, formation and characterization. *J. Controlled Release* **2012**, *161*, 473–483.
- (14) Matsumura, Y.; Maeda, H. A new concept for macromolecular therapeutics in cancer chemotherapy: mechanism of tumoritropic accumulation of proteins and the antitumor agent smancs. *Cancer Res.* **1986**, *46*, 6387–6392.
- (15) Wright, G. L., Jr.; Haley, C.; Beckett, M. L.; Schellhammer, P. F. Expression of prostate-specific membrane antigen in normal, benign, and malignant prostate tissues. *Urol. Oncol.: Semin. Orig. Invest.* **1995**, *1*, 18–28.
- (16) Yao, V.; Berkman, C. E.; Choi, J. K.; O'Keefe, D. S.; Bacich, D. J. Expression of prostate-specific membrane antigen (PSMA), increases cell folate uptake and proliferation and suggests a novel role for PSMA in the uptake of the non-polyglutamated folate, folic acid. *The Prostate* **2010**, *70*, 305–16.
- (17) Laidler, P.; Dulińska, J.; Lekka, M.; Lekki, J. Expression of prostate specific membrane antigen in androgen-independent prostate cancer cell line PC-3. *Arch. Biochem. Biophys.* **2005**, *435*, 1–14.
- (18) Yao, V.; Berkman, C. E.; Choi, J. K.; et al. Expression of prostate-specific membrane antigen (PSMA), increases cell folate uptake and proliferation and suggests a novel role for PSMA in the uptake of the non-polyglutamated folate, folic acid. *The Prostate* **2010**, *70*, 305.
- (19) Ghosh, A.; Heston, W. D. Tumor target prostate specific membrane antigen (PSMA) and its regulation in prostate cancer. *J. Cell. Biochem.* **2004**, *91*, 528–539.
- (20) Fournel, M.; Bonfils, C.; Hou, Y.; Yan, P. T.; Trachy-Bourget, M.-C.; Kalita, A.; Liu, J.; Lu, A.-H.; Zhou, N. Z.; Robert, M.-F.; et al. MGCD0103, a novel isotype-selective histone deacetylase inhibitor, has broad spectrum antitumor activity in vitro and in vivo. *Mol. Cancer Ther.* **2008**, *7*, 759–768.
- (21) Whittle, J. R.; Desai, J. Histone deacetylase inhibitors in cancer: What have we learned? *Cancer* **2015**, *121*, 1164–1167.
- (22) Varshosaz, J.; Taymouri, S.; Hassanzadeh, F.; Haghjooy Javanmard, S.; Rostami, M. Folate synperionic-cholesteryl hemisuccinate polymeric micelles for the targeted delivery of docetaxel in melanoma. *BioMed Res. Int.* **2015**, *2015*, No. 746093.
- (23) Zeng, S.; Zu Chen, Y.; Fu, L.; Johnson, K. R.; Fan, W. In vitro evaluation of schedule-dependent interactions between docetaxel and doxorubicin against human breast and ovarian cancer cells. *Clin. Cancer Res.* **2000**, *6*, 3766–3773.
- (24) NIH, National Cancer Institute, 2016. <http://www.cancer.gov/about-cancer/treatment/drugs/fda-docetaxel>.
- (25) Zhang, Q.; Sun, M.; Zhou, S.; Guo, B. Class I HDAC inhibitor mocetinostat induces apoptosis by activation of miR-31 expression and suppression of E2F6. *Cell Death Discovery* **2016**, *2*, No. 16036.
- (26) Nahire, R.; Haldar, M. K.; Paul, S.; Ambre, A. H.; Meghni, V.; Layek, B.; Katti, K. S.; Gange, K. N.; Singh, J.; Sarkar, K.; Mallik, S. Multifunctional polymersomes for cytosolic delivery of gemcitabine and doxorubicin to cancer cells. *Biomaterials* **2014**, *35*, 6482–6497.
- (27) Marsden, H. R.; Gabrielli, L.; Kros, A. Rapid preparation of polymersomes by a water addition/solvent evaporation method. *Polym. Chem.* **2010**, *1*, 1512–1518.
- (28) Traverso, N.; Ricciarelli, R.; Nitti, M.; Marengo, B.; Furfaro, A. L.; Pronzato, M. A.; Marinari, U. M.; Domenicotti, C. Role of glutathione in cancer progression and chemoresistance. *Oxid. Med. Cell. Longevity* **2013**, *2013*, No. 972913.
- (29) Jin, J.; Sui, B.; Gou, J.; Liu, J.; Tang, X.; Xu, H.; Zhang, Y.; Jin, X. PSMA ligand conjugated PCL-PEG polymeric micelles targeted to prostate cancer cells. *PLoS One* **2014**, *9*, No. e112200.
- (30) Kong, B.; Seog, J. H.; Graham, L. M.; Lee, S. B. Experimental considerations on the cytotoxicity of nanoparticles. *Nanomedicine* **2011**, *6*, 929–941.
- (31) Xu, X.; Farach-Carson, M. C.; Jia, X. Three-dimensional in vitro tumor models for cancer research and drug evaluation. *Biotechnol. Adv.* **2014**, *32*, 1256–1268.
- (32) Desoize, B.; Gimonet, D.; Jardiller, J. Cell culture as spheroids: an approach to multicellular resistance. *Anticancer Res.* **1998**, *18*, 4147–4158.
- (33) Tauskela, J. S.; Hewitt, K.; Kang, L. P.; Comas, T.; Gendron, T.; Hakim, A.; Hogan, M.; Durkin, J.; Morley, P. Evaluation of glutathione-sensitive fluorescent dyes in cortical culture. *Glia* **2000**, *30*, 329–41.
- (34) Michelet, F.; Gueguen, R.; Leroy, P.; Wellman, M.; Nicolas, A.; Siest, G. Blood and plasma glutathione measured in healthy subjects by HPLC: relation to sex, aging, biological variables, and life habits. *Clin. Chem.* **1995**, *41*, 1509–1517.